Assessment of a parabolic dish-Stirling-diesel-battery system for rural electrification: A Bolivian highland case study

***Pablo Jimenez Zabalaga*[a], *Sergio Balderrama*[a,b], *Evelyn Cardozo*[a], *Ioannis Boukas*[c]**

[a] *San Simon University, Centro Universitario de Investigacion en Energia, Cochabamba, Bolivia, p.jimenez@umss.edu.bo*

[b] *University of Liège, Energy System Research Unit - Thermodynamics Laboratory, Department of Mechanical and Aerospace Engineering, Liège, Belgium, slbalderrama@doct.uliege.be*

[c] *University of Liège, Department of Electrical Engineering and Computer Science, Liège, Belgium, ioannis.boukas@uliege.be*

ABSTRACT

In the last decades, the growing energy demand, the variability of fossil fuel prices, the depletion of oil resources and the increasing greenhouse gas emissions have been encouraging the development of affordable, sustainable and reliable technologies for power generation. Thus, an effective solution to properly integrate flexible consumption, storage devices, renewable and conventional energy sources in a decentralized manner is through the development of microgrids. In this paper, a nontraditional parabolic dish-Stirling-diesel-battery hybrid microgrid is proposed and evaluated. Referred to the components, the parabolic solar dish-Stirling engine system (PSDS) serves as the primary source of electricity generation while the diesel generator in conjunction with the battery bank provides electrical energy backup when the primary source of power is unavailable. In this way, the novelty of the study relies on a comparison between the mentioned system and conventional isolated microgrids, such as diesel-battery and PV-diesel-battery systems, using an open-source simulator of the microgrid operation. The developed model is used to study a hypothetical case of electrification for a 100-household rural village in Bolivia called Pojo Pata. The results indicate that the proposed system is very competitive compared to the other configurations. Whereas PV-diesel-battery system is still shown to have a slightly lower levelized cost of electricity (LCOE) and operational costs than the studied system, the PSDS microgrid represents about 16% of savings in terms of LCOE and 21% related to operational costs in comparison to the conventional diesel-battery system. Moreover, two control strategies for the PSDS microgrid, an optimization-based and a rule-based algorithms, are evaluated in terms of the operational costs. The optimization-based controller was able to outperform the common rule-based one, as it reached near 4% of savings.

KEYWORDS

Microgrid, Parabolic solar dish, Stirling engine, Diesel genset, Batteries.

1. INTRODUCTION

The role of electricity is fundamental for the economic and social development of a community as it has become a key commodity for daily human activities. An increase in the rate of electricity access enhances the opportunities for industrial development and improves the quality of health and education services [1]. In this context, United Nations (UN) have established the access to affordable, reliable, sustainable and modern energy for all as a sustainable development goal for its 2030 agenda [2]. In order to achieve this goal, developing countries are making strenuous efforts that include the transition from traditional centralized generation towards the introduction of a large number of distributed renewable energy resources (DERs). These systems present the opportunity to reduce losses along transmission and distribution lines when connected to lower voltage distribution lines [3]. Besides, the modularity of these systems introduces a better alternative to cover electricity requirements in remote places where the supply is technologically or financially challenging by long distances from power lines, topology or frequent outages due to severe weather conditions [4, 5]. In contrast, the aforementioned systems also face problems, including the costs of manufacturing, the slow replacement of current energy systems and the lack of adequate marketing and implementation policies [6]. Related to technical challenges, the integration of different types of technologies introduces a degree of complexity, generally in matters of operation and control of these systems [7].

Bolivian rural population is dispersed, the main electrical grid does not always extend to all populated areas and the country relies mostly on fossil fuels as its main sources of energy for electricity generation currently [8]. According to the Electricity and Nuclear Technology Control Authority (Autoridad de Fiscalización de Electricidad y Tecnología Nuclear, AETN), the installed capacity for electricity generation in the country was 3.71 GW in the country by the year 2020, out of which 72% comes from thermoelectric power stations, 20% from hydroelectric power plants and 8% from other renewable sources such as wind energy and photovoltaic systems. On the other hand, diesel, gasoline and other derivatives are fuels imported and provided at subsidized prices in the country [9]. Thus, the Bolivian government has been promoting projects to carry out a transition from the current energy mix towards distributed generation, aiming to reach 22% use of fossil fuels, 74% of hydroelectric and 4% of other types of sources renewable by the year 2025 [10]. Nevertheless, the country has a high potential for solar energy due to its position close to the equator line and its high altitude with respect to sea level, reaching an average irradiation level that exceeds the global average value [8]. Practically, 97% of the national territory is suitable for utilizing solar energy as a primary source, the 3% remaining have been identified as areas of dense cloudiness, located east of the Andes region [11]. According to the Global Solar Atlas of Bolivia, daily global horizontal irradiation in the lowlands of the country (Santa Cruz, Beni, Pando and north of La Paz) reaches a maximum of 5.1 kWh/m^2/day, while in the region of the valleys (Cochabamba, Chuquisaca and Tarija) this value varies from 5.1 to 6.7 kWh/m^2/day and in the high plateau zone (La Paz, Oruro and Potosí) the solar energy potential can fluctuate between 6.7 to 9.5 kWh/m^2/day [12].

Subsequently, technologies that harness solar power to deliver electrical energy could be divided into two broad categories: Photovoltaics (PV) and concentrating solar power (CSP). PV modules transform solar radiation directly into electricity. Nonetheless, typical commercially available silicon modules possess an efficiency in the range of 15 to 20% [13]. On the other hand, CSP systems use mirrors to concentrate sunlight and produce high-temperature heat for generating electricity. There are four types of commercial CSP technologies: Linear Fresnel reflector (LFR), parabolic-trough collector (PTC), solar central tower (SCT) and parabolic solar dish (PSD) [14]. Related to the first two types, sunlight is concentrated on a linear receiver, which usually is a tube inside a glass container for isolation and gets to temperatures of around

400 °C [15]. Moreover, solar-to-electric efficiencies of these technologies are between 8% and 18%, which are highly related to the energy density due to concentration and geometrical characteristics (Concentration ratio) [16]. For the rest of the types of PSDS (SCT,PSD), sunlight is concentrated to a point receiver, which reaches temperatures of around 800 °C (PSD) and 600-1200 °C (SCT) [17]. Furthermore, their solar-to-electric efficiencies vary from 20% to 30%, which include all systems components such as the steam turbine or Stirling engine [16]. In this manner, the parabolic solar dish Stirling (PSDS) systems have been considered as the most efficient systems used to convert solar energy to electricity among all solar technologies (29.4% of efficiency) [18]. Additionally, the Stirling engine has been analyzed through the years and has been considered as a promising technology for remote electrification due to its versatility of fuels, simple mechanism, low noise, low environmental impact, theoretical high efficiency and easy maintenance [19, 20].

2. LITERATURE REVIEW

2.1. Microgrids with RES

Microgrids are small-scale electrical grids composed of different generators that harness both renewable and fossil-fueled technologies along with storage systems and flexible consumption. The operation of these type of systems is carried out locally and their distribution is usually not regulated [21]. Thus, their energy management system (EMS) provide the key to ensure reliable, economical and safe operation through the application of a control approach. A vast number of studies of microgrids have targeted electricity generation in remote rural areas [22–24]. Moreover, papers of systems focusing on developing countries have established their advantages, such as minimizing energy costs and being able to meet load requirements year-round [25, 26]. Some studies have looked at microgrids that integrate technologies such as PV modules, wind turbines, battery banks, and internal combustion engines, using mostly HOMER (Hybrid Optimization Model for Electric Renewables) software for modeling [27–29].

2.2. Microgrids with CSP technologies

Solar thermal power is considered ideal technology to hybridize with other energy technologies for energy generation. CSP could also be integrated with technology related to conventional power generation into a synergistic system, leading to many potential benefits including improved dispatchability and reliability, increased efficiency, lowered capital costs through equipment sharing, and the opportunity to reach flexible operation by alternating between energy sources. In this way, the energy sources that a CSP could incorporate include coal, natural gas, biofuels, geothermal energy, and wind energy [30]. Zhai et al. [31] proved that a PTC-coal power plant was able to reduce the overall CSP plant cost, representing only be 72% of the cost of a stand-alone solar plant and generated over 25% more electricity. Zhang et al. [32] evaluated a dual source boiler configuration, where a SCT was utilized in parallel with a coal-fired boiler to supplement its heat. Their design demonstrated a high solar-to-electric efficiency of 27.8%, while a common stand-alone parabolic trough plant might only achieve approximately between 15 to 20% efficiency. Mokheimer et al. [33] assessed a STC combined with a gas turbine system that could heat air to approximately 1000 ºC. Moreover, a heat recovery steam generator (HRSG) was used to produce steam in a cogeneration setting, reaching an instantaneous solar share of 74.2% and an annual solar share of 31.5%. Other study analyzed a linear LFR system with direct steam generation in conjunction with a fluidized bed biomass boiler, which had an efficiency of 32.5% and an investment cost that was 69% lower than a stand-alone CSP system [34]. Ayub et al. [35] performed an analysis using a PTC-geothermal system with an organic Rankine cycle. Their findings showed that hybridization decreased LCOE by 2%, while the optimization of a geothermal plant could reduce LCOE by 8%. Vick and Moss [36], showed that PTC technology was a match with a wind turbine to meet the electrical load in the Texas and proposed a mix of 67% wind with 33% CSP for that area. Although the hybrid was more expensive (on an LCOE basis) than a pure wind farm, it had better ability to meet peak demand than a pure wind farm. Ghosh and Dincer explored using a multi-generation system based on solar-wind-geothermal configuration in order to generate electricity, cooling, water purification, process drying, and space heating [37].

2.3. Microgrids with PSDS

Although PSDS systems are suitable for hybridization [38], few research works have addressed their integration with other technologies. Furthermore, no literature has been found that assess the implementation of an isolated PSDS-diesel-battery microgrid for power generation, since most of the studies have focused on the modeling and simulation of hybrid power systems that includes a parabolic dish and a wind turbine. Most of the aforementioned studies have focused on modeling and simulation of a PSDS-wind turbine system. Shariatpanah et al. [39] introduced a new connected hybrid microgrid configuration, which was composed of a PSDS system and a small wind turbine [39]. The results of this study indicated that the configuration provided a high performance compared to other microgrids, based on modeling of the electrical components, controllers and loads in Simulink to verify voltage stability. Rahman et al. [40], analyzed the automatic generation control of a hybrid PSDS-WT system by assessing the generation rate and speed governor dead band constraint. Shboul et al. [41], conducted a techno-economic analysis of a new PSDS-WT system and compare this configuration with the tradicional PV-WT system for power generation. The article established that the system was very competitive with a LCOE between 0.13 and 0.15 USD/kWh, and an approximate hourly cost of 4 USD/h. Other study by Kadri and Hadj Abdallah, performed a technical performance analysis related to an isolated PSDS-battery system located in the coasts of Tunisia [42]. The whole work analyzed the microgrid through various solar radiation conditions during the year and showed that the EMS proposed was very efficient and allowed a balance between the solar generation and battery subsystems due to the maintenance of the voltage of the DC bus with respect to its reference value. Wu et al. [43] evaluated a hybrid system based on steam-air biomass gasification integrated with PSDS system for trigeneration. The authors conclude that this novel configuration obtains an total energy efficiency of 51.34%. Mastropasqua et al. [44] have studied the hibridization of PSDS system with a solid oxide electrolysis cell to produce electricity, thermal energy and hydrogen. The study showed that the system can be operated at a nominal solar-to-hydrogen efficiency of above 30% producing 30 kWe and 150 kg/day of hydrogen.
As a result of reviewing the latest literature, it was shown that there is a gap in the research of microgrids that include PSDS as part of their configuration. Moreover, most of the papers had evaluated large scale commercial PSDS configurations and almost no attention has been given to small scale standalone PSDS systems [45]. The present study aims at filling this knowledge gap and adopts a comprehensive approach in assessing the proposed novel system.

3. METHODS

This research addresses the techno-economic assessment of a PSDS-diesel-battery microgrid as compared to a hybrid PV-diesel-battery and a diesel-battery systems since these are common solutions for power generation in rural areas. A study case was presented and took into account the electric load of a rural community in Bolivia named Pojo Pata. Moreover, the completion of the work lead to evaluate two dispatch strategies (Rule-based and MPC algorithms) for the studied hybrid power system. Due to the complexity of hybrid microgrids, two software were selected, one for sizing (HOMER) and the other for simulation of microgrids (MicrogridRLsimulator). HOMER is a computational model for micropower solutions designed by the National Renewable Energy Laboratory (NREL). It assists the user to find the optimized group of architectures that satisfy the technical limitations at the lowest net present cost [46]. MicrogridRLsimulator is an open source simulator of off-grid microgrid operation developed in Python, which contains a detailed modelling of components, such as storage, consumption,steerable and non-steerable generators. Also, it allows for applying any control strategy and receives as input the components size and parameters, time series representing the exogenous information, and simulation parameters [47].

The paper has proposed a methodology that started with an economic optimization. Next, a modeling approach of the different components was developed using the defined mathematical equations in MicrogridRLsimulator and adding the modelling of the Dish-Stirling engine system, which includes the optical and heat transfer phenomena related to its functioning. After that, two simulations of the systems were carried out, one through the worst day in solar radiation and the other through an entire year. Finally, the performance analyses were executed by considering the levelized cost of energy (LCOE) and total cost of operation of the different microgrid configurations and control strategies. Hence, the methodology and general approach of the current study is presented in Figure 1.

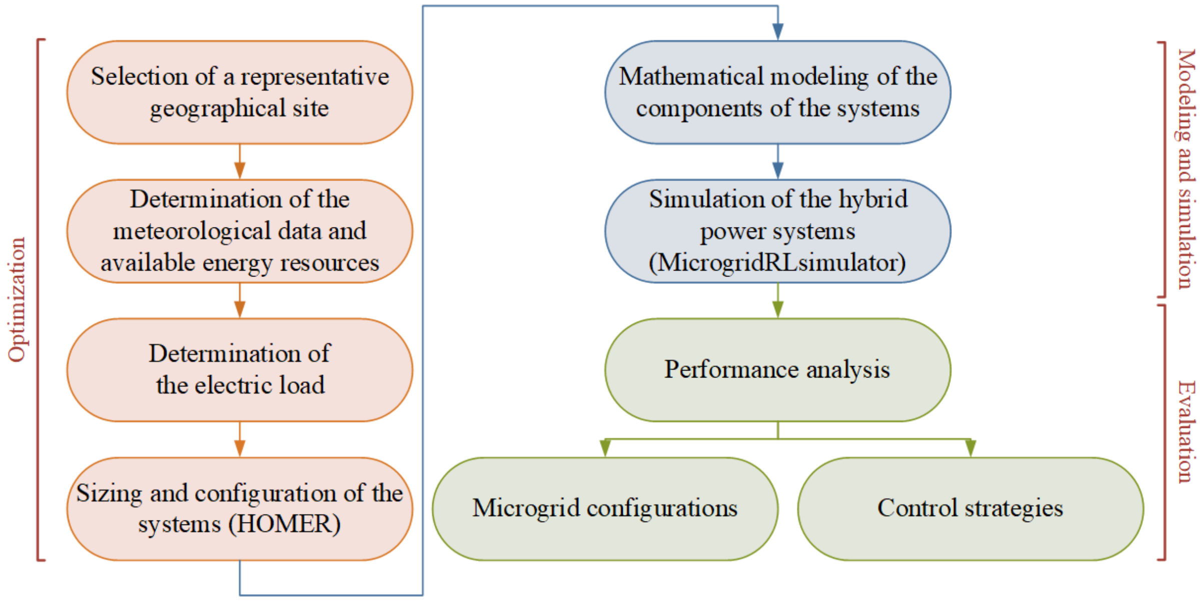

Figure 1. Methods and general approach of system analysis.

4. CASE STUDY

The following sections present a detailed description of meteorological data, load demands, components and their respective costs related to a standalone Parabolic dish-Stirling-Diesel-battery system.

4.1. Geographical site selection

According to the latest population and household census of Bolivia performed in 2012, the departments with the lowest electrification rate were Chuquisaca (69%), Potosí (71%) and Pando (72%), where the major part of that percentages were concetrated in rural areas. [48]. The gap between urban and rural electricity access is bigger as a consequence of losses in the transmission and distribution, which affects the cost of power grid extension [49]. Consequently, a community located at Potosí that had largest number of households without access to electricity was selected. Therefore, the chosen village was Pojo Pata with an electrification rate of less than 5% of total households, relying most of the time on the use of small diesel generators [48].

4.1.1. Geographic and demographic characteristics

Pojo Pata is situated in Potosí, 42 kilometers north of its capital (-19.197, -65.744). Its average altitude above sea level is 3532 m, that leads to a climate characterized by low temperatures [50]. The principal economic activity is agriculture and the community has a population of 451 inhabitants and 100 households which were estimated by the year 2021 [48].

4.2. Climatological characteristics

This community has a high average annual solar radiation due to its location in Altiplano, which is a highland region in Bolivia. It has an estimated average direct normal solar radiation of 6.85 kWh/m^2/day, with variations between 5.47 kWh/m^2/day in winter and 8.18 kWh/m^2/day in summer [51, 52]. Figure 2 presents monthly average direct normal solar radiation of this community.

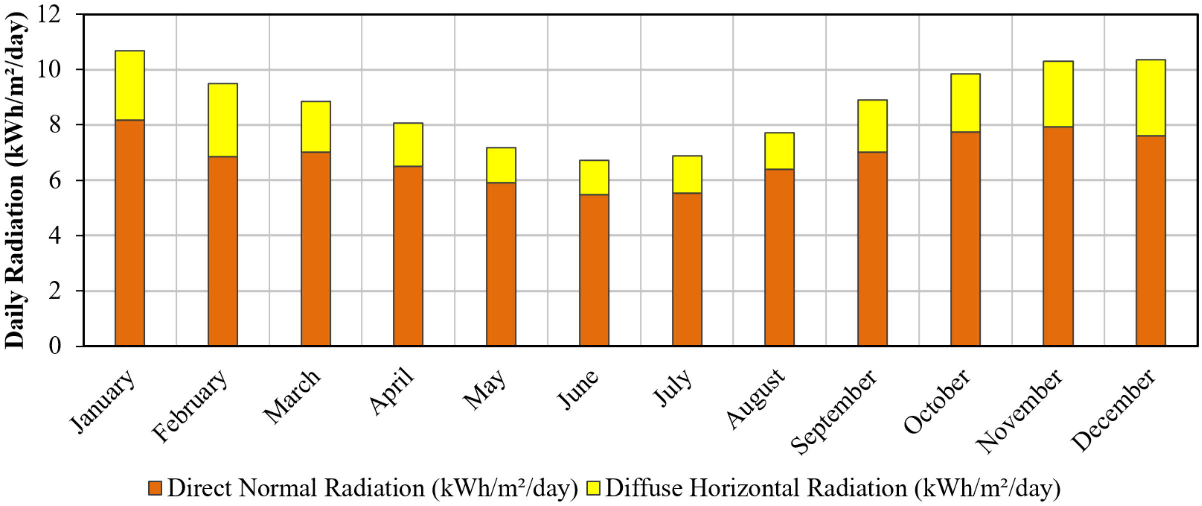

Figure 2. Monthly average solar radiation data in Pojo Pata.

The dry and cold climate of this community is a consequence of scarce fluvial precipitation and the presence of the eastern part of Andes mountain, which acts as a barrier to the flow of humid air from the Atlantic Ocean and the Amazon Basin [53]. The average annual temperature is 13.3 °C, and extreme temperatures are between 10.1 °C and 15.3 °C, in the cold and hot seasons respectively, as indicated in Figure 3.

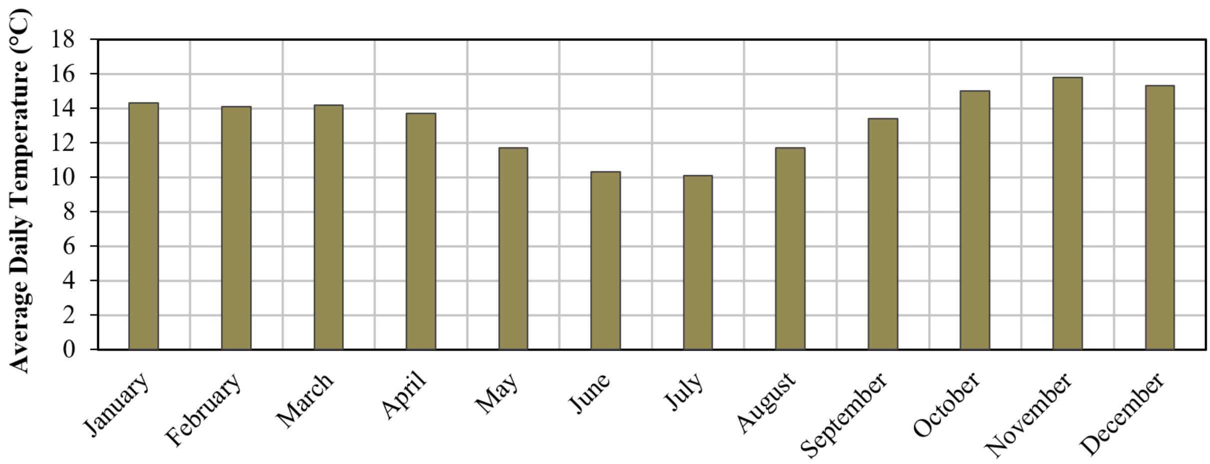

Figure 3. Monthly average temperature data in Pojo Pata.

4.3. Electric energy consumption

Pojo Pata's electricity demand is based on a previous study to a community with similar characteristics, located in the Altiplano zone and done by Fernandez et al. [54].The mentioned work contemplated villages composed of inhabitants of low and high incomes, a school, a health center, public lighting and a church. The generated daily load profiles are provided in Figure 4.

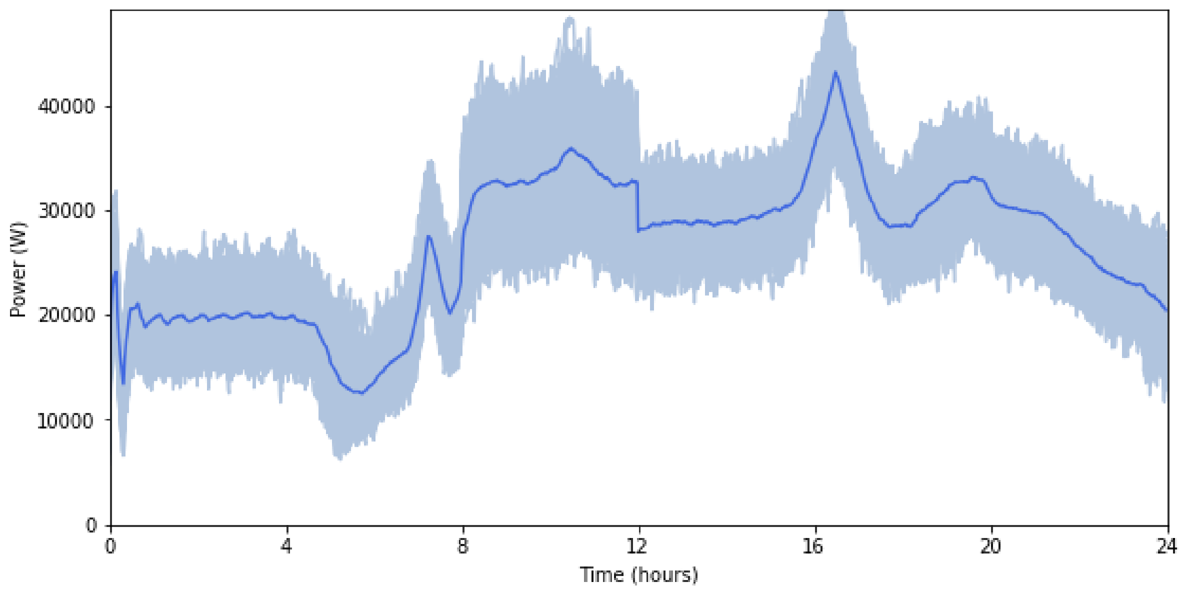

Figure 4. Monthly-averaged daily load profile in Pojo Pata [55].

4.4. Configurations

The architecture of all systems was based on a centralized AC bus because this configuration allows the development of modular systems, which can adapt to potential changes in the consumption. These systems are also considered robust and easier to operate [56]. Furthermore, the AC bus architecture permits an easier interconnection with a power grid when this is required [57]. Related to the the different microgrids, diesel-battery systems are the most common configuration of isolated systems in Bolivia [10]. Moreover, due to the concern related to the diesel subsidy, the Bolivian government has been promoting projects for the hybridization of these remote plants using PV panels (PV-diesel-battery systems). In this way, the micro-grids of Cobija and El Espino are examples of this trend [58, 59]. The configurations of the PSDS-diesel-battery, PV-diesel-battery and Diesel-battery systems are shown in Figure 5.

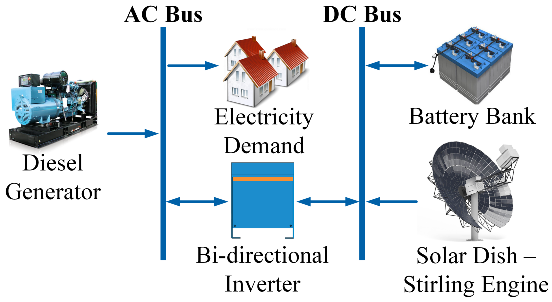

(a) PSDS-Diesel-battery system.

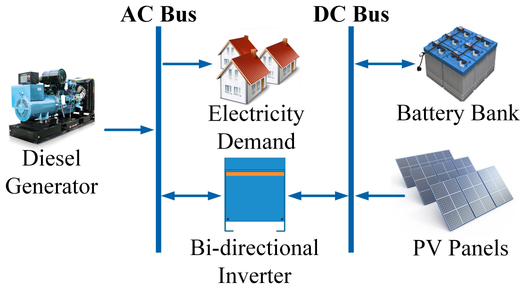

(b) PV-Diesel-battery system.

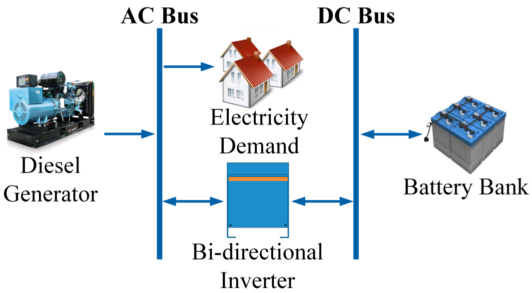

(c) Diesel-battery system.

Figure 5. Overall configuration of the microgrids.

4.5. Techno-economic data

In this section, specifications of the diverse components and their costs are expressed. Moreover, an extensive literature review was carried out in order to acquire data about the local costs of the equipment used.

4.5.1. PV panels

Technical characteristics of the PV module that constituted the photovoltaic array were based on a 320 Wp one [60]. Additionally, a tracking system was not considered. The slope and azimuth angles were selected in order to maximize the yearly electricity generation and ended up as 19.197° (latitude of site) and 180° (module facing north), respectively [61]. The ground reflectance was considered as wet soil from the city [62] and the derating factor was 88%, which was the default value defined in HOMER. This last factor considers different types of losses in the PV modules such as aging, shading, soiling, and wiring losses [63]. The capital cost and replacement cost of the mentioned PV panel were 747 and 344 USD, respectively [64]. Additionally, prices relating to shipping, installation, and a solar inverter were included in the capital cost. The O&M cost of the 320 W photovoltaic module studied was assumed to be 18 USD/year.

4.5.2. Battery bank

The main characteristics of each battery were: A 12 VRLA-GEL battery with a nominal capacity of 200 Ah and a lifetime throughput of 690 cycles [65]. Due to the voltage of 24 V related to

DC bus, the batteries were configured in series of two batteries per string. Furthermore, the depth of discharge (DOD) of the battery was taken as 80%, due to the fact that the manufacturer specified that this type of battery offers a better deep cycle durability and a longer lifetime than AGM batteries [65]. The capital cost and replacement cost of each battery were 793 and 703 USD, respectively and 14 USD/year was established (2% of acquisition cost) as the O&M cost [66].

4.5.3. Converter

As a consequence of both DC and AC buses existing in the system, a bi-directional inverter, which has both function of a rectifier and an inverter, performed the conditioning of the system and was based on Victron MultiPlus Inverter [67]. The lifetime of the equipment was assumed to be 15 years, based on the software default value [68] and the efficiency of the inverter and rectifier were taken as 94% and 98%, according to the manufacturer's datasheet [69]. The capital and replacement cost of the converter were assumed to be 1,764 and 1,604 USD, respectively. The O&M cost was established as 160.4 USD/year (1% of acquisition cost) [66].

4.5.4. Diesel engine genset

The capital cost, the replacement cost, and the O&M cost of the diesel generator were assumed to be 925 USD/kW, 804 USD/kW, and 0.0124 USD/kW/year, respectively. The minimum load ratio was taken as 30% of the nominal power and the generator operating hours were considered as 20,000 [70]. Furthermore, diesel fuel was specified with a price of 1.30 USD/L and the default properties of that fuel in the library of the optimization program (lower heating value 43.20 MJ/kg and density 820 kg/m3) [71].

4.5.5. Parabolic solar dish-Stirling engine system

According to Shboul et al. [41], a solar powered Stirling engine has an investment cost around 2,861.5 USD/kW, a replacement cost of 2,271 USD/kW and an O&M cost of 57.6 USD/kW/year. Related to the life expectancy of the system, the manufacturer expresses that it has a lifetime of around 30 years. [72] The other parameters demanded from the aforementioned system were based on the technical characteristics of the Eurodish system, which is a demonstration project, located in Spain and composed of a SOLO Stirling engine V161 with a maximum electrical output of 10 kW [73].

4.5.6. Other parameters

The lifetime of the project was taken as 20 years, the nominal discount rate was selected as 10.10% [9], the expected inflation rate was expressed as 3.12% [74] and the annual capacity shortage was assumed to be 0%. Furthermore, some important parameters related to the use of MicrogridRLsimulator are expressed in Table 1.

4.6. Mathematical Modeling

In this section, a detailed description of the system considered is provided. The considered microgrid is composed of a solar dish Stirling engine, a diesel genset, a battery bank, a charge controller, an inverter and a electric load. The Energy Management System (EMS) is responsible for the interaction and the scheduling of the controllable components. A PSDS system is composed of the following components:

4.6.1. Consumption

In this paper, an electric load of a rural Bolivian village (C^t) was considered non-flexible, which is related to a high cost associated to non-served energy. In this way, the demand at each time-

Table 1. Input parameters for the simulation.

Parameter	Value	Unit
$\overline{P}$,$\underline{P}$	0.72	kW × battery
η^{ch}	87.65	%
η^{dis}	84.08	%
π^{fuel}	1.21	EUR/kWh
π^{curt}	1.50	EUR/kWh
π^{shed}	2.00	EUR/kWh
Δ_t	1	h

step t came from distribution $P_{\mathrm{t}}^{\mathrm{C}}$[75].

4.6.2. Dish-Stirling Engine

The Dish-Stirling engine system incorporates three mainly components: Parabolic dish concentrator, solar receiver and Stirling engine coupled with an electrical generator. The direct normal irradiation (DNI) is collected and reflected by the parabolic dish into the receiver, which is designed to transfer the absorbed solar energy to the working fluid in Stirling engine. The Stirling engine then converts absorbed thermal energy to mechanical power. Finally, the linear motion is converted to a rotary motion to turn a generator to generate electricity.

4.6.2.1. Opto-geometric model

The interception factor (ϕ_{fi}), which is the fraction of energy entering into the receiving cavity and is calculated by the following relation [76]:

$$\phi_{fi} = 1 - \exp(\frac{1}{2 \cdot C \cdot {\sigma_f}^2}) \tag{1}$$

In this way, the lost energy outside the cavity aperture area is deduced from the interception factor. Let σ_f denote the error of the distribution of heat flux in the focal plane, C is the concentration factor defined as $C = A_{con}/A_{ap}$, where A_{con} is the projected reflective surface of the solar parabolic dish concentrator and A_{ap} is the aperture surface of the receiving cavity.

4.6.2.2. Thermal analysis model

The thermal power received by the aperture surface of the receiving cavity is given by the following equation [77],

$$Q_{rec} = I \cdot A_{con} \cdot \eta_{op} \cdot \phi_{fi} \tag{2}$$

where η_{op} is the optical efficiency of the solar parabolic dish concentrator which is defined as the product of the coefficient of absorptivity, emissivity, and transmissivity of the concentrator, I is the direct normal irradiation. The thermal input power to the Stirling Engine (Q_u) is estimated by subtracting the receiver thermal losses from the power intercepted by the receiver as exemplified in the equation below [7],

$$Q_u = Q_{rec} - Q_{rad,ref} - (Q_{cond} + Q_{conv} + Q_{rad,emit}) \tag{3}$$

where the terms include reflected radiation ($Q_{rad,ref}$), emitted radiation losses ($Q_{rad,emit}$), total convection losses (Q_{conv}), which includes both natural and forced convection, and conduction losses (Q_{cond}).

4.6.2.3. Stirling engine

The performance of Stirling engine could be evaluated through Beale number, which is based on numerous Stirling engines and estimate the output power, which is shown in Equation 4 [78,79].

$$P^{gross} = B \cdot P_m \cdot V_{SW} \cdot f \tag{4}$$

Here P^{gross} is the gross output power of the engine, B is the Beale number, P_m is the mean engine pressure, V_{SW} is the swept volume of the engine and f is the engine frequency. Beale number is a parameter that characterizes the performance of Stirling engine and lies between the range from 0.11 to 0.15 for engines that function with high temperature differential [80]. On the other hand, the net system power (P^{net}) is obtained by subtracting the parasitic power of the tracking motors, control system, pump, and fan from the gross output value. These parasitic losses reach an average value of 350 W during the operation of the PSDS system and a value of 10 W when the engine is off as a consequence of the uninterruptible power supply that the control system must have [72].

4.6.3. Diesel genset

The diesel generator operates at output level of ${P^{gen}}_t$ that is ranging between the minimum stable generation $\underline{P^{gen}}$ and the maximum capacity $\overline{P^{gen}}$ such that:

$$\underline{P^{gen}} \leq {P^{gen}}_t \leq \overline{P^{gen}} \tag{5}$$

The fuel consumption F_t related to the operation of the generator at time t is a function of the power output ${P^{gen}}_t$ with parameters F_1, F_2 given by the manufacturer.

$$F_t = \begin{cases} F_1 + F_2 \cdot {P^{gen}}_t & \text{,if } {P^{gen}}_t > 0, \\ 0 & \text{,otherwise.} \end{cases} \tag{6}$$

The fuel cost ${c^{fuel}}_t$ accounting for the fuel price π^{fuel} is then given by:

$${c^{fuel}}_t = F_t \cdot \pi^{fuel} \tag{7}$$

4.6.4. Battery bank

The battery bank is based on a linear tank model. Therefore, the dynamics of a battery are given by the following expressions [75]:

$$SOC_{t+1} = SOC_t + \Delta t \cdot (\eta^{ch} P^{ch} t - \frac{P^{dis} t}{\eta^{dis}}) \tag{8}$$

$$SOC_t, P^{ch} t, P^{dis} t \geq 0 \tag{9}$$

$$P^{ch} t \leq \overline{P} \tag{10}$$

$$P^{dis} t \leq \underline{P} \tag{11}$$

$$SOC_t \leq \overline{S} \tag{12}$$

$$\overline{S} = s(n_t) \tag{13}$$

Where SOC_t represents the state of charge at each time step t, P^{ch} and P^{dis} denote the charging and discharging power, respectively. Moreover, $\overline{P}$ and $\underline{P}$ are the maximum charging and discharging rates, $\overline{S}$ is the maximum battery capacity, η^{ch} and η^{dis} are the charging and discharging efficiencies and n_t the number of cycles.

4.7. Power balance

At each time step t, the power balance is defined as [75]:

$$P^{net}{}_t + P^{dis}{}_t + P^{shed}{}_t = P^{ch}{}_t + P^{curt}{}_t + C_t \tag{14}$$

Where P^{shed} is the shedding of loads and P^{curt} is the curtailment of generation.

4.7.1. Control Strategies

In this paper, two different control approaches for microgrid operation have been implemented for comparison purposes: Rule-based and optimization-based control.

4.7.1.1. Rule-based controller

The rule-based control strategy is simple and implements a set of rules that are considered each time step using data regarding the present state of the system. The basic principle of controller is to use the renewable generation in order to supply the electrical power demand [75]. Thus, the residual generation (ΔP_t) is defined as the subtraction between the power produced from renewable resources ($P^{res}{}_t$) and the demand of power (C_t). Thus, if there is an excess of electricity generation ($\Delta P_t > 0$), then this will be used to charge the batteries. On the other hand, if the residual generation level is negative ($\Delta P_t < 0$), the batteries can supply the demand. Nonetheless, prior evaluation, the actual state of charge of the batteries should be revised (SOC) and there are certain limits of charge ($\overline{P}$) and discharge rates ($\underline{P}$). A complete description of this algorithm is presented in Figure 6.

4.7.1.2. Optimization controller

Optimization-based algorithms, such as the model predictive control (MPC), are not common in industrial applications. They allow to harness optimization techniques and enable reaching multiple control objectives simultaneously. A MPC is used to establish control actions at each time step by solving an optimization problem with N-step look-ahead. In this way, the objective function tries to minimize the curtailment, load shedding and fuel cost subject to the constrains of operation which are defined by a mixed-integer linear model [75]. The optimization problem that is solved at each current state of the system as exemplified in the flowchart in Figure 7.

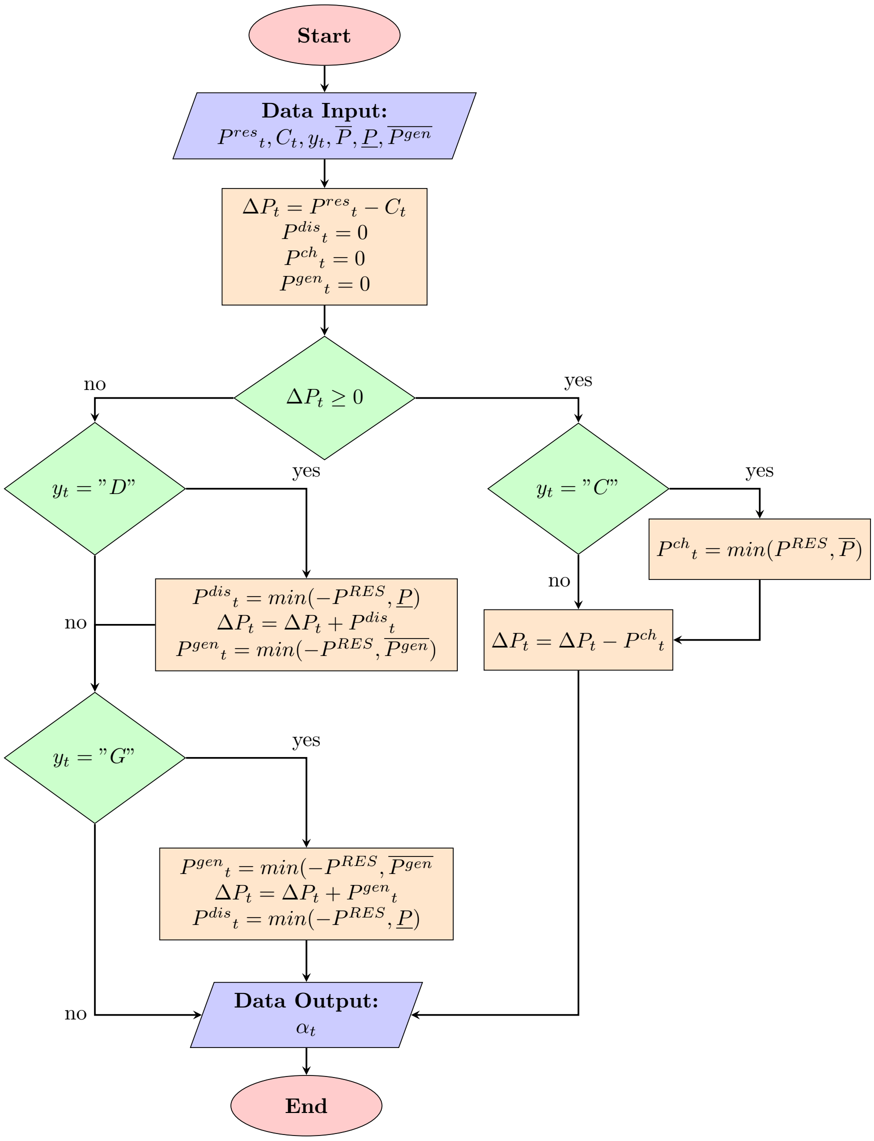

Figure 6. Flowchart of the rule-based control algorithm.

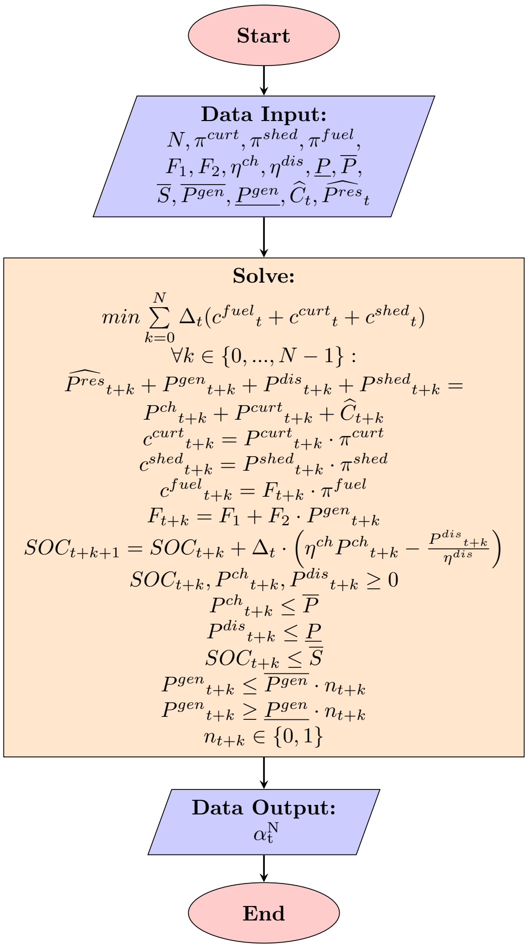

Figure 7. Flowchart of the optimization control algorithm.

5. VALIDATION

As the reviewed literature showed, there are not studies that reflect the real performance of a PSDS-diesel-battery system nor simulated one. Nonetheless, a validation of the hybrid power system components was performed before they can be used to study the performance of the actual systems.

5.1. PSDS system

In order to validate the model presented, data from Eurodish system located in Sevilla for an entire day (November 1st, 2007) were evaluated in comparison to the developed model. Figure 8 exemplifies that Beale number model is considerably good in comparison to the real data, especially during central hours of the day. Nevertheless, real energy generation during the start-up is higher than the estimated due to overpressure. Meanwhile, there was a manually shut-down at the end of the day by the team of operation and maintenance [72]. Although these discrepancies, the Beale model is surprisingly adjusted to the real behavior of the system with a mean absolute error (MAE) of 59.17 W and a mean absolute percentage error (MAPE) of 0.30%.

5.2. Other components

Referred to PV modules, battery storage, diesel generator and bi-directional inverter, Totaro et al. performed an evaluation and validation of an isolated PV-diesel-battery microgrid based on empirical data measured in the community of El Espino (19.188, 63.560), Bolivia [75].

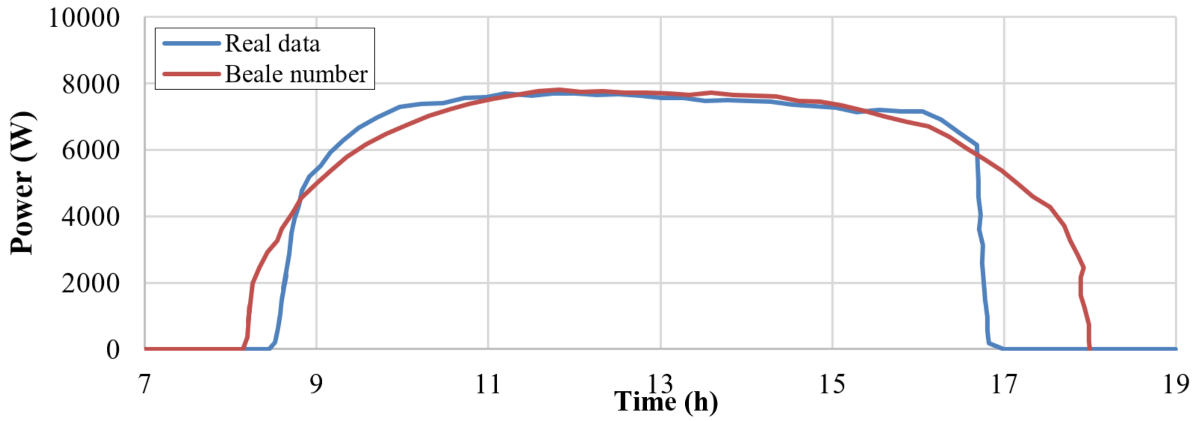

Figure 8. Comparison between the values of Eurodish system vs Beale number model [72].

6. RESULTS AND DISCUSSION

In this section, the results of the paper are presented. In the first part, the optimization results are analysed and after that, the analysis of microgrid simulation are described.

6.1. Optimization results

Optimization results expressed the following microgrid components' sizing:

1. Configuration 1 (PSDS case) — PSDS systems (6 × 10 kW), diesel genset (35 kW), bi-directional inverter (40 kW), and VRLA gel lead-acid battery bank (26 × 2.4 kWh).

2. Configuration 2 (PV case) — PV panels (204 × 0.32 kW), diesel generator (30 kW), bi-directional inverter (36 kW), and VRLA gel lead-acid battery bank (40 × 2.4 kWh).

3. Configuration 3 (Diesel case) — Diesel generator (45 kW), bi-directional inverter (0.43 kW), and VRLA gel lead-acid batteries (6 $\times$ 2.4 kWh).

6.2. Microgrids' simulation

For the interest of this article, it was considered to first simulate the systems for a representative solar radiation day (Worst day of solar energy) and, then, for an entire year using microgridRL-simulator [75]. Unsurprisingly, the selected day (July 23^{rd}) was a cloudy day in winter season. In this way, the one-day approach was done in order to corroborate whether the systems operate in a reliable, efficient way. Moreover, the one-year simulation was completed in order to obtain the data needed for the performance analysis.

6.2.1. Analysis of the microgrid configurations during a representative solar day

On July 23^{rd}, as shown in Figure 9, the electrical generation by solar technologies occurred from 07:00 a.m. to 06:00 p.m. Nevertheless, the RES production from the PSDS-diesel-battery system (PSDS case) (Figure 9a) was lower than the PV panels (PV case) (Figure 9b) as a consequence of the lower DNI during a cloudy day. On the other hand, a one-hour load shedding took place around 4:00 p.m and had the same value for both mentioned systems, which was easily covered by the system composed of a diesel genset and a battery bank (Diesel case) (Figure 9c). Moreover, PV case registered another load shedding at 07:00 p.m., which was smaller than the previous one. Regarding the battery bank, the Diesel case did not required to use it; quite the contrary the system was able to recharge the batteries at 05:00 a.m. While PSDS case need a discharge process at 04:00 a.m. during one hour and PV case required two discharges of the batteries (At 12:00 a.m. and at 04:00 a.m.). To sum up, the results of this daily simulation showed that all microgrids functioned properly, but PSDS case and PV case were not able to cover the electricity demand once and twice during the day, respectively. Nonetheless, all the components functioned coordinately to reach the load required.

6.2.2. Analysis of the microgrid configurations during a year

PSDS case was able to reduce 16% (0.446 USD/kWh) the levelized cost of energy (LCOE) in comparison to the Diesel case (0.531 USD/kWh). Nevertheless, PV case represented the lowest LCOE solution (0.426 USD/kWh) from the three configurations. With regards to cumulative returns, PV case also yields the best alternative with 55,920 € for an entire year. PSDS case and Diesel case reached 87,205 and 110,259 €, respectively. Additionally, PSDS system, which for a total installed capacity of 60 kW, was able to generate 151,023 kWh and reached a average solar-to-electric efficiency of 22.3%. In contrast, the 65.28 kWh PV array generated 128,249 kWh during the entire year with an average solar-to-electric efficiency of 14.9%.

From the previous results, it is clearly seen that the use PSDS system can reduce LCOE and operational costs compared to only using a diesel genset as a steerable generator in a microgrid. Nevertheless, Stirling engine has a main drawback related to its manufacturing costs that could about twice the price of a diesel engine [81]. This fact has lead PV panels to still be the best option for solar-power systems even if the site such as the case of Pojo Pata has an excellent solar potential (2819 kWh/m^2/year), which is 1.5 times bigger than the potential recommended by the literature and experimental projects implemented using solar dishes [82, 83]. Furthermore, the local fabrication and availability of the technology could lower the prices as some works have reported with LCOE values varying from 0.13 USD/kWh in Pakistan [45], 0.26 USD/kWh in China [84], 0.83 USD/kWh in Malaysia [85] and 0.24 USD/kWh in Algeria [86]. Therefore, the feasibility of PSDS generation systems will also depend on technology costs, project costs, and the extent of government driven financial support [87].

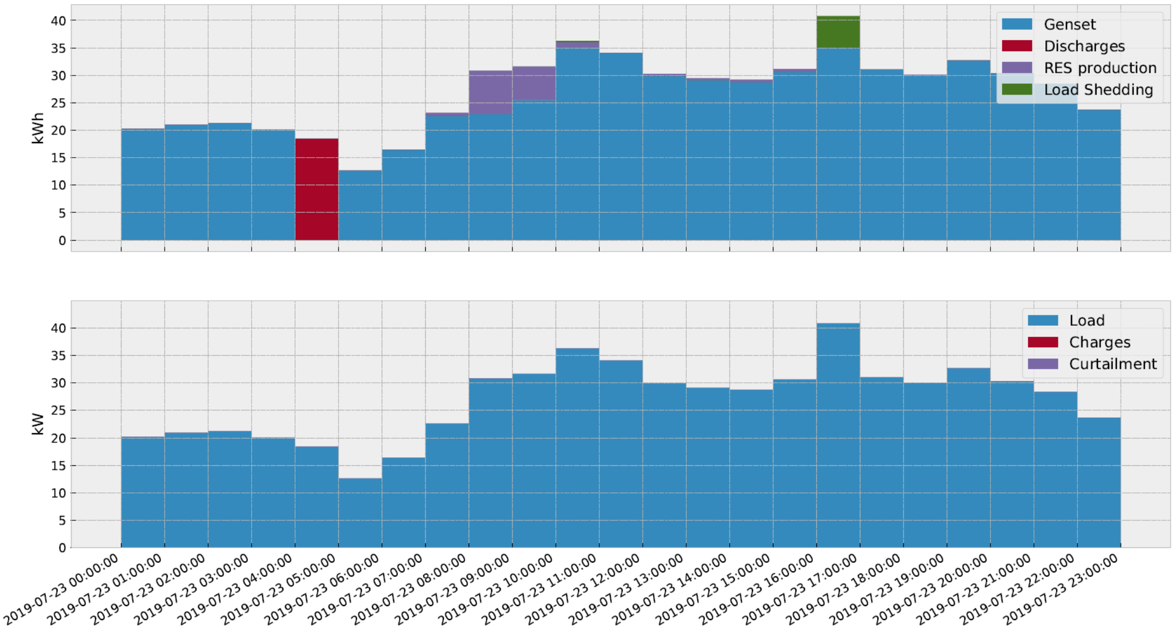

(a) Configuration 1 — PSDS case.

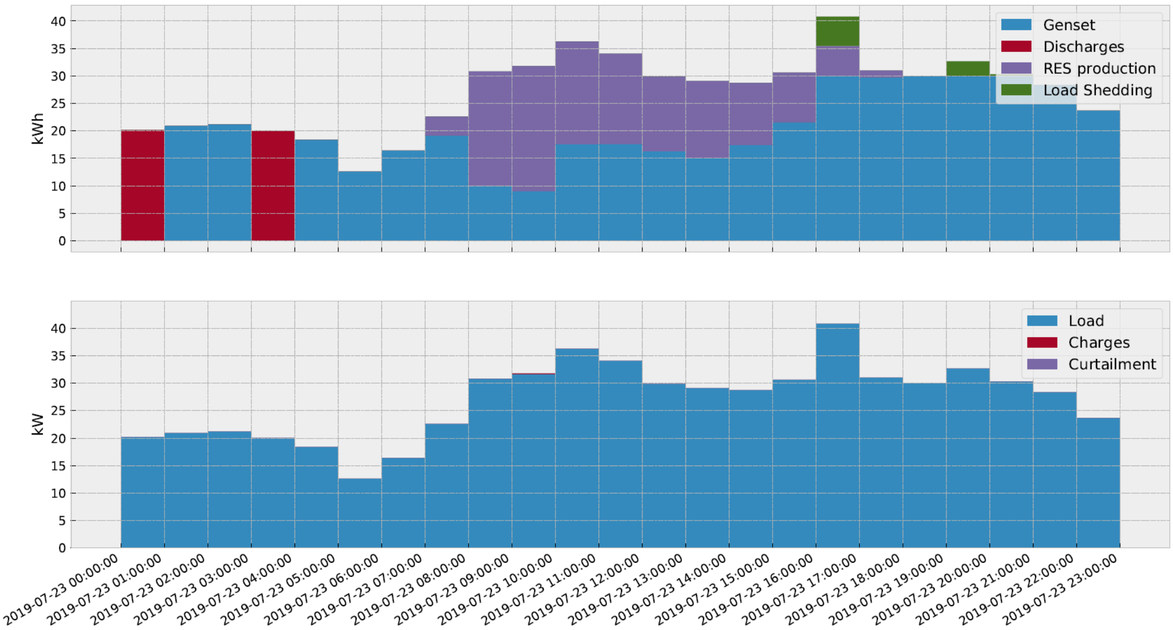

(b) Configuration 2 — PV case.

Figure 9. Generated power of the different microgrids on July 23rd in Pojo Pata.

6.2.3. Analysis of the control strategies during a representative solar day

A rule-based controller, which is typically found in industrial applications of microgrids, was compared against an optimization controller with perfect knowledge and 12 periods of look-ahead for PSDS case. Thus, as it is possible to observe in Figure 10, the MPC algorithm maximize the use of the diesel generator in order to charge the batteries with the excess energy (01:00 a.m.-04:00 a.m., 07:00 a.m.-08:00 a.m., 01:00 p.m.-04:00 p.m., 05:00 p.m.-06:00 p.m. and 08:00 p.m.-11:00 p.m.) and discharge them to cover the demand leading to a non-load shedding during the entire day in comparison to the typical rule-based controller used in Figure 9a. Related to RES production, both controllers were limited to the weather conditions of that day, generating the same amount of power from the PSDS system.

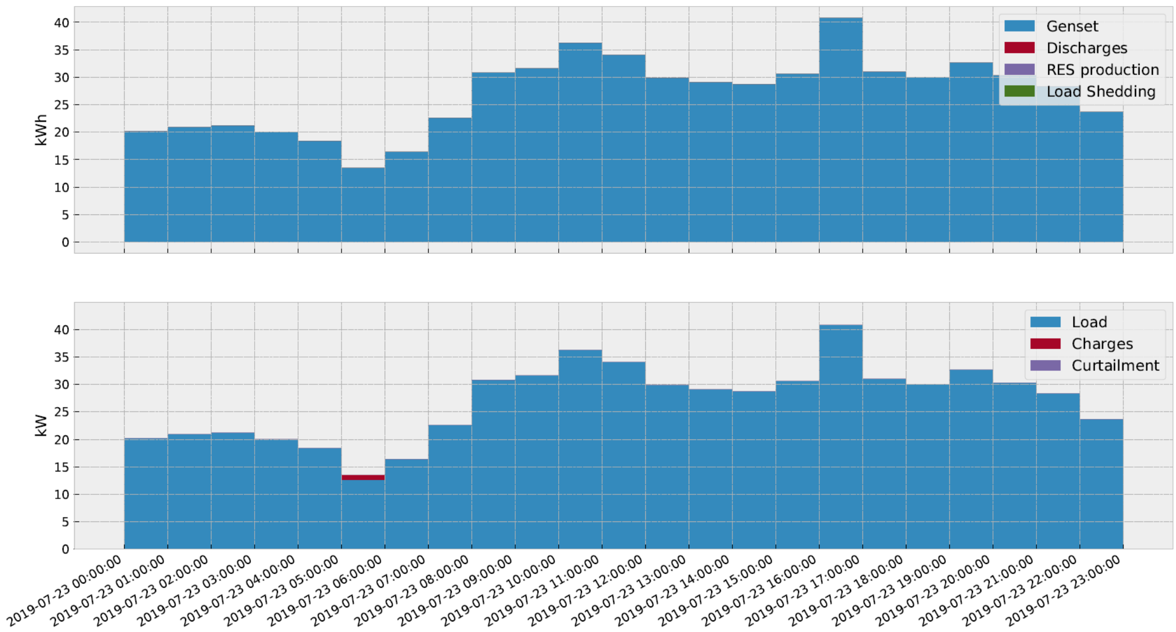

(c) Configuration 3 — Diesel case.

Figure 9. Generated power of the different microgrids on July 23^{rd} in Pojo Pata.

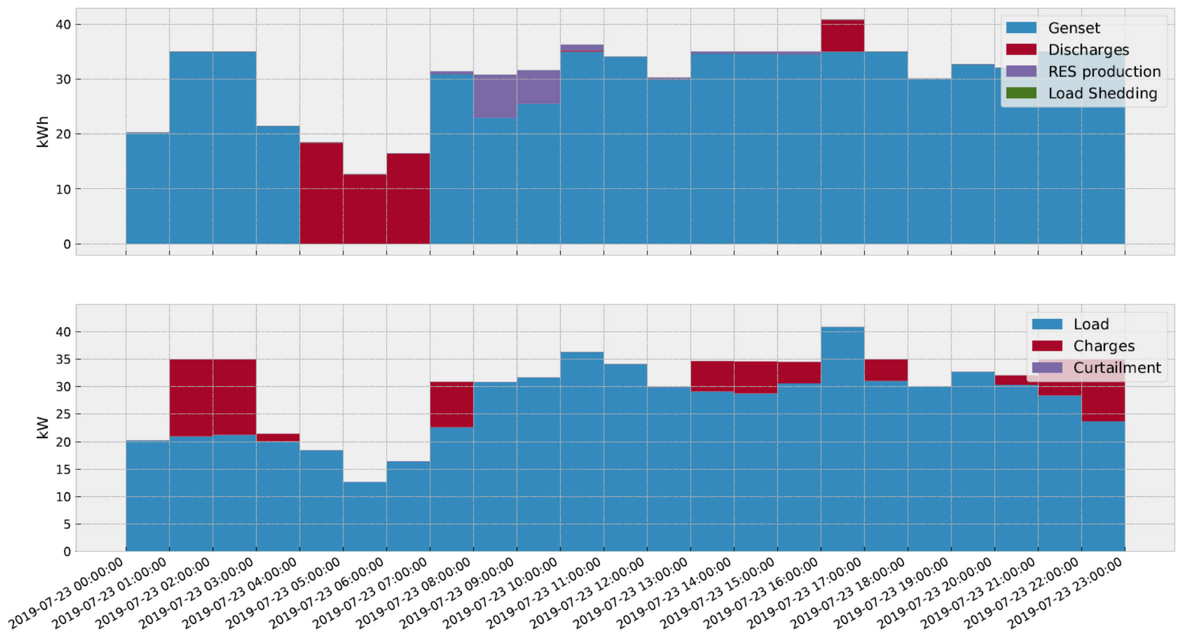

Figure 10. Generated power of PSDS case using an MPC algorithm (Optimization controller) on July 23^{rd} in Pojo Pata.

6.2.4. Analysis of the control strategies during a year

In addition to evaluating the effectiveness of a PSDS-diesel-battery system in comparison to other common microgrids, another goal of this paper is to conduct a comparative study between different control strategies from the point of view of minimizing the operational costs. In this way, the MPC method (83,499 EUR) approximately yields a saving of 4.25% for an entire year in comparison to the rule-based method (87,205 EUR). The operating cost savings reached are due to a better control and integration of the different components of the microgrid as it has been reported in the previous section. So, it can be observed that the use of an optimization-based controller is indeed able to significantly reduce the cost related to the functioning of the system. Nevertheless, the results obtained were based on a perfect forecast, which is not the case in real applications. The incorporation of uncertainties in forecasting models is out of the scope of this article.

7. CONCLUSIONS

In this paper, a comprehensive study of a novel remote hybrid microgrid (PSDS-Diesel-battery system) was presented. First, a detailed description of meteo data and techo-economic data related to the rural community of Pojo Pata is presented in order to use that information as input for HOMER software, which led to techno-economically optimized configurations.
Subsequently, components of the system were modeled using mathematical models previously reported in the literature. Each model considers important factors of the evaluated technology such as the model of the Parabolic dish-Stirling engine which considered three main components involving opto-geometric and thermal characteristics. Moreover, an open-source framework for the simulation of power grid was utilized [75].
Then, a comparison between the mentioned system and other common standalone power system configurations was performed. Although the standalone PSDS-diesel-battery system was not as cheap as the PV-diesel-battery system, it represented around 21% of operational savings in comparison to the diesel-battery system. Additionally, the difference between LCOEs of the PSDS case and the PV case was minimal.
Finally, an assessment of two different control strategies for the PSDS case was performed. The model-predictive controller (MPC) was able to outperform the common rule-based controller, as it reached near 4% of savings. Despite the high purchase price of the Stirling engine, the hybrid system based on a parabolic dish, Stirling engine, diesel genset and batteries for the community of Pojo Pata represented a better option to implement in a rural electrification project compared to a system made up of diesel generator and batteries. There is a great opportunity for systems based on Stirling engines to benefit users of distributed energy systems, as this technology matures, and more developments are made. Moreover, the policy measures are required to rise the financial attraction and decrease the investment costs of PSDS systems for the competitiveness with other concentrated solar power technologies. Further research should be directed to assess other control strategies that utilize artificial intelligence. Moreover, an evaluation of impact of uncertainties on the forecasting models and a multi-energy system to generate electricity and heat for the community should be considered.

Nomenclature

Functions

$P_{\mathrm{t}}^{\mathrm{C}}$ Load probability distribution

Parameters

Δ_t Simulation and control period duration (h)

η^{ch} Charging efficiency of battery bank

η^{dis} Discharging efficiency of battery bank

η_{gen} Electrical efficiency of generator

η_{op} Optical efficiency of parabolic dish concentrator

$\overline{P^{gen}}$ Maximum capacity of Diesel genset (kW)

$\overline{P}$ Maximum charging rate of battery bank (kW)

$\overline{S}$ Maximum battery capacity (kWh)

ϕ_{fi} Interception factor

π^{curt} Curtailment price (EUR/kWh)

π^{fuel} Fuel price (EUR/kWh)

π^{shed} Load shedding price (EUR/kWh)

σ_f Error of the distribution of heat flux in the focal plane

$\underline{P^{gen}}$ Minimum stable generation of Diesel genset (kW)

$\underline{P}$ Maximum discharging rate of battery bank (kW)

$\widehat{C}$ Load forecast (kW)

$\widehat{P^{res}}$ Renewable generation forecast (kW)

A_{ap} Aperture surface of receiving cavity (m^2)

A_{con} Projected reflective surface of parabolic dish (m^2)

B Beale number

C Concentration factor

f Stirling engine frequency (Hz)

F_1 Fuel consumption parameter of diesel genset

F_2 Fuel consumption parameter of diesel genset

N Number of look-ahead periods

P_m Mean Stirling engine pressure (Pa)

V_{SW} Displaced Stirling engine volume (m^3)

Set and indices

k Look-ahead step

t Decision time step

Variables

α_t Control actions vector

ΔP_t	Residual generation level (kW)
c^{curt}	Curtailment cost (EUR)
c^{fuel}	Fuel cost (EUR)
c^{shed}	Lost load cost (EUR)
C_t	Electric load at each time-step t (kW)
F_t	Fuel consumption of diesel genset (l)
I	Direct Normal Irradiation(W/m^2)
n_t	Number of cycles of battery
P^{ch}	Charging power of battery bank (kWh)
P^{dis}	Discharging power of battery bank (kWh)
P^{gross}	Gross output power of Stirling engine (W)
P^{net}	Net output power of Stirling engine (kW)
Q_{cond}	Conduction losses (W)
Q_{conv}	Convection losses (W)
$Q_{rad,emit}$	Emitted radiation losses (W)
$Q_{rad,ref}$	Reflected radiation losses (W)
Q_{rec}	Thermal power at receiving cavity (W)
Q_u	Thermal input power to the Stirling Engine (W)
SOC_t	State of charge of battery bank at each time step (kWh)
SOC_{t+1}	State of charge of battery bank at next time step (kWh)
y_t	Discrete decision about the use of the equipment
${c^{fuel}}_t$	Fuel cost related to Diesel genset (EUR)
${P^{curt}}_t$	Curtailment of generation (kW)
${P^{gen}}_t$	Power output of Diesel genset (kW)
${P^{res}}_t$	Renewable generation (PSDS or PV panels) (kW)
${P^{shed}}_t$	Shedding of loads (kW)

REFERENCES

[1] World Bank, *World Development Report 2021: Data for Better Lives*. The World Bank, 2021.

[2] F. F. Nerini, J. Tomei, L. S. To, I. Bisaga, P. Parikh, M. Black, A. Borrion, C. Spataru, V. C. Broto, and G. Anandarajah, "Mapping synergies and trade-offs between energy and the Sustainable Development Goals," *Nature Energy*, vol. 3, no. 1, pp. 10–15, 2018.

[3] E. Colombo, S. Bologna, and D. Masera, *Renewable energy for unleashing sustainable development*. Milan: Springer, 2013.

[4] N. El Bassam, "Renewable energy for rural communities," *Renewable Energy*, vol. 24, no. 3-4, pp. 401–408, 2001.

[5] S. Chowdhury, S. P. Chowdhury, P. Crossley, and The Institution of Engineering and Technology, "Microgrids and Active Distribution Networks," tech. rep., Londres, 2009.

[6] S. Chu and A. Majumdar, "Opportunities and challenges for a sustainable," *Nature*, vol. 488, no. 7411, pp. 294–303, 2012.

[7] D. Rekioua, *Hybrid Renewable Energy Systems: Optimization and Power Management Control*. Springer Nature, 2019.

[8] M. Fernandez, C. Fernandez, and G. Rodriguez, "Situación Energética de Bolivia y Desafíos," tech. rep., Cochabamba, 2020.

[9] Inter-American Development Bank, "Evaluación Financiera y Económica del Proyecto Electrificación Rural con Energía Renovable (BO-X1013)," tech. rep., Cochabamba, 2013.

[10] Autoridad de Fiscalización de Electricidad y Tecnología Nuclear, "Anuario Estadístico 2020," tech. rep., Autoridad de Fiscalización de Electricidad y Tecnología Nuclear, La Paz, Bolivia, 2020.

[11] M. Fernandez, "Estudio sostiene que la energía solar es factible en el 97

[12] M. Lucano and I. Fuentes, "Atlas de la Distribución Solar en Bolivia," tech. rep., Universidad Mayor de San Simón (UMSS), Cochabamba, Bolivia, 2010.

[13] R. Everett, S. Peake, and J. Warren, *Energy systems and sustainability: Power for a sustainable future*. Oxford University Press, 3rd ed., 2021.

[14] A. G. Fernández, J. Gomez-Vidal, E. Oró, A. Kruizenga, A. Solé, and L. F. Cabeza, "Mainstreaming commercial CSP systems: A technology review," *Renewable energy*, vol. 140, pp. 152–176, 2019.

[15] J. Twidell and T. Weir, *Renewable energy resources*. London: Routledge, 3rd ed., 2015.

[16] W. Van Sark and B. Corona, "Chapter 12 - Concentrating solar power," pp. 221–231, Academic Press, 2020.

[17] M. T. Islam, N. Huda, A. B. Abdullah, and R. Saidur, "A comprehensive review of state-of-the-art concentrating solar power (CSP) technologies: Current status and research trends," *Renewable and Sustainable Energy Reviews*, vol. 91, pp. 987–1018, 2018.

[18] V. Punnathanam and P. Kotecha, "Effective multi-objective optimization of Stirling engine systems," *Applied Thermal Engineering*, vol. 108, pp. 261–276, 2016.

[19] A. C. Bachelier, "Stirling engines A technology overview," *Research Paper*, pp. 1–37, 2009.

[20] I. Arashnia, G. Najafi, B. Ghobadian, T. Yusaf, R. Mamat, and M. Kettner, "Development of micro-scale biomass-fuelled CHP system using Stirling Engine," *Energy Procedia*, vol. 75, pp. 1108–1113, 2015.

[21] J. G. P. Balderrama, S. B. Subieta, F. Lombardi, N. Stevanato, A. Sahlberg, M. Howells, E. Colombo, and S. Quoilin, "Incorporating high-resolution demand and techno-economic optimization to evaluate micro-grids into the Open Source Spatial Electrification Tool (OnSSET)," *Energy for Sustainable Development*, vol. 56, pp. 98–118, 2020.

[22] M. Muralikrishna and V. Lakshminarayana, "Hybrid (solar and wind) energy systems for rural electrification," *ARPN Journal of Engineering and Applied Sciences*, vol. 3, no. 5, pp. 50–58, 2008.

[23] A. H. Munthe, "A Hybrid Renewable Energy System for a Rural Area in Africa," 2009.

[24] S. Mandelli, J. Barbieri, R. Mereu, and E. Colombo, "Off-grid systems for rural electrification in developing countries: Definitions, classification and a comprehensive literature review," *Renewable and Sustainable Energy Reviews*, vol. 58, pp. 1621–1646, 2016.

[25] P. Nema, R. K. Nema, and S. Rangnekar, "A current and future state of art development of hybrid energy system using wind and PV-solar: A review," *Renewable and Sustainable Energy Reviews*, vol. 13, no. 8, pp. 2096–2103, 2009.

[26] A. J. Organ, *Stirling cycle engines: Inner workings and design*. John Wiley Sons, 2013.

[27] S. M. Shaahid, I. El-Amin, S. Rehman, A. Al-Shehri, J. Bakashwain, and F. Ahmad, "Potential of autonomous/off-grid hybrid wind-diesel power system for electrification of a remote settlement in Saudi Arabia," *Wind Engineering*, vol. 28, no. 5, pp. 621–627, 2004.

[28] S. G. Sigarchian, R. Paleta, A. Malmquist, and A. Pina, "Feasibility study of using a biogas engine as backup in a decentralized hybrid (PV/wind/battery) power generation system–Case study Kenya," *Energy*, vol. 90, pp. 1830–1841, 2015.

[29] S. Bahramara, M. P. Moghaddam, and M. R. Haghifam, "Optimal planning of hybrid renewable energy systems using HOMER: A review," *Renewable and Sustainable Energy Reviews*, vol. 62, pp. 609–620, 2016.

[30] K. M. Powell, K. Rashid, K. Ellingwood, J. Tuttle, and B. D. Iverson, "Hybrid concentrated solar thermal power systems: A review," *Renewable and Sustainable Energy Reviews*, vol. 80, pp. 215–237, 2017.

[31] R. Zhai, C. Li, Y. Chen, Y. Yang, K. Patchigolla, and J. E. Oakey, "Life cycle assessment of solar aided coal-fired power system with and without heat storage," *Energy conversion and management*, vol. 111, pp. 453–465, 2016.

[32] M. Zhang, X. Du, L. Pang, C. Xu, and L. Yang, "Performance of double source boiler with coal-fired and solar power tower heat for supercritical power generating unit," *Energy*, vol. 104, pp. 64–75, 2016.

[33] E. M. A. Mokheimer, Y. N. Dabwan, and M. A. Habib, "Optimal integration of solar energy with fossil fuel gas turbine cogeneration plants using three different CSP technologies in Saudi Arabia," *Applied Energy*, vol. 185, pp. 1268–1280, 2017.

[34] J. H. Peterseim, U. Hellwig, A. Tadros, and S. White, "Hybridisation optimization of concentrating solar thermal and biomass power generation facilities," *Solar Energy*, vol. 99, pp. 203–214, 2014.

[35] M. Ayub, A. Mitsos, and H. Ghasemi, "Thermo-economic analysis of a hybrid solar-binary geothermal power plant," *Energy*, vol. 87, pp. 326–335, 2015.

[36] B. D. Vick and T. A. Moss, "Adding concentrated solar power plants to wind farms to achieve a good utility electrical load match," *Solar Energy*, vol. 92, pp. 298–312, 2013.

[37] S. Ghosh and I. Dincer, "Development and analysis of a new integrated solar-wind-geothermal energy system," *Solar energy*, vol. 107, pp. 728–745, 2014.

[38] S. Guo, Q. Liu, J. Sun, and H. Jin, "A review on the utilization of hybrid renewable energy," *Renewable and Sustainable Energy Reviews*, vol. 91, pp. 1121–1147, 2018.

[39] H. Shariatpanah, M. Zareian Jahromi, and R. Fadaeinedjad, "Simulation of a new grid-connected hybrid generation system with Stirling engine and wind turbine," *Journal of Renewable and Sustainable Energy*, vol. 5, no. 6, p. 63128, 2013.

[40] A. Rahman, L. C. Saikia, and N. Sinha, "Automatic generation control of an interconnected two-area hybrid thermal system considering dish-stirling solar thermal and wind turbine system," *Renewable energy*, vol. 105, pp. 41–54, 2017.

[41] B. Shboul, A.-A. Ismail, S. Michailos, D. Ingham, O. H. AL-Zoubi, L. Ma, K. Hughes, and M. Pourkashanian, "Design and Techno-economic assessment of a new hybrid system of a solar dish Stirling engine instegrated with a horizontal axis wind turbine for microgrid power generation," *Energy Conversion and Management*, vol. 245, p. 114587, 2021.

[42] Y. Kadri and H. H. Abdallah, "Performance evaluation of a stand-alone solar dish Stirling system for power generation suitable for off-grid rural electrification," *Energy Conversion and Management*, vol. 129, pp. 140–156, 2016.

[43] H. Wu, Q. Liu, Z. Bai, G. Xie, J. Zheng, and B. Su, "Thermodynamics analysis of a novel steam/air biomass gasification combined cooling, heating and power system with solar energy," *Applied Thermal Engineering*, vol. 164, p. 114494, 2020.

[44] L. Mastropasqua, I. Pecenati, A. Giostri, and S. Campanari, "Solar hydrogen production: Techno-economic analysis of a parabolic dish-supported high-temperature electrolysis system," *Applied Energy*, vol. 261, p. 114392, 2020.

[45] A. A. Lashari, P. H. Shaikh, Z. H. Leghari, M. I. Soomro, Z. A. Memon, and M. A. Uqaili, "The performance prediction and techno-economic analyses of a stand-alone parabolic solar dish/stirling system, for Jamshoro, Pakistan," *Cleaner Engineering Technology*, vol. 2, p. 100064, 2021.

[46] F. A. Farret and M. G. Simões, *Integration of renewable sources of energy*. John Wiley Sons, 2017.

[47] I. Boukas, *Deep Reinforcement Learning for the Control of Energy Storage in Grid-Scale and Microgrid Applications*. PhD thesis, Université de Liège - ULiège > Dép. d'électric., électron. et informat. (Inst.Montefiore) > Smart grids, 2021.

[48] Instituto Nacional de Estadística, "Censo Nacional de Población y Vivienda 2012," 2012.

[49] B. Branisa, L. E. Andersen, M. Cardona, and N. Zegarra, "L-Luz eléctrica," *INESAD book chapters*, vol. 1, pp. 131–137, 2016.

[50] VYMaps, "Pojo Pata, Potosí," 2021.

[51] S. Pfenninger and I. Staffell, "Long-term patterns of European PV output using 30 years of validated hourly reanalysis and satellite data," *Energy*, vol. 114, pp. 1251–1265, 2016.

[52] R. Gelaro, W. McCarty, M. J. Suárez, R. Todling, A. Molod, L. Takacs, C. A. Randles, A. Darmenov, M. G. Bosilovich, and R. Reichle, "The modern-era retrospective analysis for research and applications, version 2 (MERRA-2)," *Journal of climate*, vol. 30, no. 14, pp. 5419–5454, 2017.

[53] R. Andressen, M. Monasterio, and L. F. Terceros, "Regímenes climáticos del altiplano sur de Bolivia: una región afectada por la desertificación," *Revista geográfica venezolana*, vol. 48, no. 1, pp. 11–32, 2007.

[54] M. Fernández, E. Cardozo, J. Zambrana, G. Peña, S. L. Balderrama Subieta, C. Sánchez, S. Soto, and S. Quoilin, "Evaluación del costo de electrificación rural en Bolivia para alcanzar el ODS 7," *Journal Boliviano de Ciencias*, 2021.

[55] M. Fernández Fuentes, E. Cardozo, J. Zambrana Vargas, G. Peña, S. L. Balderrama Subieta, C. Sánchez, A. Soto, and S. Quoilin, "Evaluación del costo de electrificación rural en Bolivia," 2020.

[56] Y. J. Reddy, Y. V. P. Kumar, K. P. Raju, and A. Ramsesh, "Retrofitted hybrid power system design with renewable energy sources for buildings," *IEEE Transactions on Smart Grid*, vol. 3, no. 4, pp. 2174–2187, 2012.

[57] O. Palizban and S. Mekhilef, *Hybrid Systems Control: with Renewable Energy Sources*. LAP LAMBERT Academic Publishing, 2012.

[58] ENDE Guaracachi, "Planta Solar Cobija," 2018.

[59] Ministerio de Comunicación de Bolivia, "Gobierno Lleva Energía eléctrica a Comunidad Guaraní "El Espino", en el Chaco Cruceño," 2018.

[60] TRINA SOLAR, "Módulo TSM-PD14," 2016.

[61] J. R. Balfour, M. Shaw, and N. B. Nash, *Advanced photovoltaic installations*. Jones Bartlett Publishers, 2011.

[62] E. Birhuett García, *Aprovechamiento de la Energía Solar Entre los Trópicos: Energía Fotovoltaica Para Ingenieros*. Cochabamba, Bolivia: ENERGÉTICA, 2016.

[63] HOMER Energy LCC, "PV Derating Factor," 2021.

[64] ENERSOL S.A., "ENERSOL Tienda," 2021.

[65] Shenzhen Center Power Tech, “VRLA Vision CG12-200PEX,” 2014.

[66] M. Hernández Arrondo, “Análisis de factibilidad de la implantación de sistemas aislados híbridos eólicos-diesel en comunidades rurales remotas de Bolivia. Diseño de un sistema de este tipo en una comunidad boliviana en la que resulte factible,” 2012.

[67] Victron Energy, “Victron MultiPlus Inverter/Charger,” 2014.

[68] HOMER Energy LCC, “Converter,” 2021.

[69] Victronenergy, “Technical notes on output rating, operating temperature and efficiency.”

[70] Finning International Inc., “Technical Information C1.5 Diesel Generator Set 2017,” tech. rep., Vancouver, Canada, 2017.

[71] HOMER Energy LCC, “Fuels,” 2021.

[72] J. M. Gavilán Conde, *Desarrollo de modelo de comportamiento del sistema disco parabólico Eurodish*. PhD thesis, 2011.

[73] M. H. Babikir, V. S. Chara-Dackou, D. Njomo, M. Barka, M. Y. Khayal, D. R. K. Legue, and J. P. Gram-Shou, “Simplified modeling and simulation of electricity production from a dish/Stirling system,” *International Journal of Photoenergy*, vol. 2020, 2020.

[74] Banco Central de Bolivia, “Indicadores de Inflación Anual,” 2021.

[75] S. Totaro, I. Boukas, A. Jonsson, and B. Cornélusse, “Lifelong Control of Off-grid Microgrid with Model-Based Reinforcement Learning,” *Energy*, p. 121035, 2021.

[76] M. Bensafi, S. Zegnoun, and B. Draoui, “Etude Expérimentale Et Modélisation D’un Concentrateur Parabolique Solaire Dans La Région De Béchar,” 2010.

[77] J. Ruelas, N. Velázquez, and J. Cerezo, “A mathematical model to develop a Scheffler-type solar concentrator coupled with a Stirling engine,” *Applied Energy*, vol. 101, pp. 253–260, 2013.

[78] G. Walker, “Elementary design guidelines for Stirling engines,” *American Chemical Society*, 1979.

[79] G. Walker, “Stirling engines,” *Clarendon Press*, 1980.

[80] P. Fraser, *Stirling Dish System Performance Prediction Model*. PhD thesis, University of Wisconsin-Madison, 2008.

[81] O. Taki, K. S. Rhazi, and Y. Mejdoub, “A Study of Stirling Engine Efficiency Combined with Solar Energy,”

[82] A. Thiam, C. Mbow, M. Faye, P. Stouffs, and D. Azilinon, “Assessment of hybrid concentrated solar power-biomass plant generation potential in Sahel: Case study of Senegal,” *Natural Resources*, vol. 8, no. 8, pp. 531–547, 2017.

[83] L. Crespo, “Chapter 13 - The long-term market potential of concentrating solar power systems,” in *Woodhead Publishing Series in Energy* (K. Lovegrove and W. B. T. C. S. P. T. S. E. Stein, eds.), pp. 477–509, Woodhead Publishing, 2021.

[84] M. E. Zayed, J. Zhao, W. Li, A. H. Elsheikh, Z. Zhao, A. Khalil, and H. Li, "Performance prediction and techno-economic analysis of solar dish/stirling system for electricity generation," *Applied Thermal Engineering*, vol. 164, p. 114427, 2020.

[85] K. Bataineh and Y. Taamneh, "Performance analysis of stand-alone solar dish Stirling system for electricity generation," *International Journal of Heat and Technology*, vol. 35, no. 3, pp. 498–508, 2017.

[86] M. Abbas, B. Boumeddane, N. Said, and A. Chikouche, "Dish Stirling technology: A 100 MW solar power plant using hydrogen for Algeria," *International journal of hydrogen energy*, vol. 36, no. 7, pp. 4305–4314, 2011.

[87] S. Stökler, C. Schillings, and B. Kraas, "Solar resource assessment study for Pakistan," *Renewable and Sustainable Energy Reviews*, vol. 58, pp. 1184–1188, 2016.